

Anticorrelation between the splitting and polarization of the exciton fine structure in single self-assembled InAs/GaAs quantum dots

Chia-Hsien Lin,¹ Wen-Ting You,¹ Hsiang-Yu Chou,¹ Shun-Jen Cheng,¹ Sheng-Di Lin,² and Wen-Hao Chang^{1,*}¹*Department of Electrophysics, National Chiao Tung University, Hsinchu 300, Taiwan*²*Department of Electronics Engineering, National Chiao Tung University, Hsinchu 300, Taiwan*

(Received 30 September 2010; revised manuscript received 16 December 2010; published 28 February 2011)

We report on a systematic correlation between the fine-structure splitting and polarization anisotropy of excitons in InAs/GaAs quantum dots, but with an unexpected reversal in order of the polarization eigenaxes. Such an anticorrelation is explained by a large valence-band-mixing induced splitting due to the shape and strain anisotropies. The strength and phase of valence band mixing are also found to play an important role in the tuning of fine structure splitting using an in-plane magnetic field.

DOI: [10.1103/PhysRevB.83.075317](https://doi.org/10.1103/PhysRevB.83.075317)

PACS number(s): 78.67.Hc, 78.55.Cr

I. INTRODUCTION

The biexciton-exciton cascade process in semiconductor quantum dots (QDs) has been considered as a promising source of entangled photon pairs¹⁻⁷ for quantum cryptography⁸ and quantum teleportation.⁹ Practical applications, however, are limited by the fine-structure splitting (FSS) in the intermediate bright exciton state due to the anisotropic electron-hole exchange interactions.¹⁰ To erase the “which path” information in the radiative cascade, tremendous effort has been made to reduce the FSS by applying external perturbations, including magnetic field,^{2,11,12} electric field,¹³⁻¹⁶ and uniaxial stress¹⁷⁻¹⁹. Although entanglement has been successfully restored by a number of tuning schemes,^{2,16} the underlying tuning mechanisms remain far from clear, due to the lack of a detail understanding of the key factors controlling FSS in QDs.

The physical origins of FSS in QDs have been elucidated theoretically either within the framework of envelop function approximation^{20,21} or based on the atomistic pseudopotential approach.^{22,23} In general, FSS in QDs is a consequence of symmetry reduction. Two main sources of in-plane asymmetry have been recognized: (i) the *intrinsic* atomistic asymmetry of the underlying lattice and (ii) the *extrinsic* dot shape asymmetry due to a preferential elongation developed during QD growth. The atomistic asymmetry can lead to a nonzero built-in FSS even in a shape-symmetric dot.²² The asymmetric shape, on the other hand, induces a nonzero long-range exchange splitting when the exciton envelop function shows in-plane asymmetry.^{20,21} Besides, a reduced symmetry will allow mixing of isospin states of heavy and light holes in the valence band.^{22,24-26} This mixing will further contribute a splitting into FSS due to the exchange interaction coupled via the light-hole admixture.^{22,25} All of the aforementioned effects on FSS are closely related to the size, shape, and composition profile of individual dots, which are, however, poorly known due to the quite limited information available from morphological techniques. Since it is also unlikely to access both the structural asymmetry and the optical spectra for each dot embedded in host materials, experimental verifications of the correlation between FSS and structural asymmetry of QDs are still absent thus far.

In this work we present an alternative approach to access both FSS and in-plane asymmetry of individual dots via

measurements of optical anisotropy.²⁴⁻²⁸ We show that FSS and polarization anisotropy of exciton in InAs/GaAs self-assembled QDs are correlated, but with an unexpected reversal in order of the polarization eigenaxes. Such an *anticorrelation* indicates that the splitting induced by the exchange interactions coupled via valence-band mixing (VBM) play an important role in the excitonic FSS in elongated QDs. The effect of an in-plane magnetic field on VBM and hence the tuning of FSS is also discussed.

II. EXPERIMENT

The QD sample was grown by molecular beam epitaxy.²⁹ A layer of InAs self-assembled QDs (2.0 monolayers) was grown on GaAs at 480°C without substrate rotations, yielding a gradient in dot density on the wafer ranging from 10^8 to 10^{10} cm⁻². The QDs were finally capped by a 100-nm undoped GaAs layer. A layer Al metal mask with arrays of apertures ($\phi \sim 1-2$ μ m) was fabricated on the sample surface for isolating single QD emissions. Single dot spectroscopy was performed in a micro-photoluminescence (μ PL) setup combined with a 6-T super-conducting magnet. The PL signals were analyzed by a 0.75-m grating monochromator combined with a liquid-nitrogen-cooled charge-coupled device (CCD) camera. Polarization-resolved measurements were carried out by using a linear polarizer combined with a half-wave retarder. The system has been carefully calibrated, such that polarization artifacts arising from the anisotropic responses of all optical components used can be excluded. By using Lorentzian lineshape fittings to the exciton peaks and sinusoidal fittings to the polarization-dependent intensity, the FSS, major polarization axis, and linear polarization degree can be determined with accuracy better than ± 5 μ eV, $\pm 2^\circ$, and $\pm 2\%$, respectively.

III. RESULTS AND DISCUSSION

Figure 1 shows polarized PL spectra of three different QDs. Each exciton (*X*) line consists of a doublet $|x\rangle$ and $|y\rangle$, with linear polarization eigenaxes close to the $[110]$ (x) and $[\bar{1}\bar{1}0]$ (y) crystallographic axes ($\pm 5^\circ$). The FSS, $\Delta_{FS} \equiv E_x - E_y$, range from +100 to -30 μ eV and vary from dot to dot. Each *X* line also exhibits polarization anisotropy. For QD-A, the

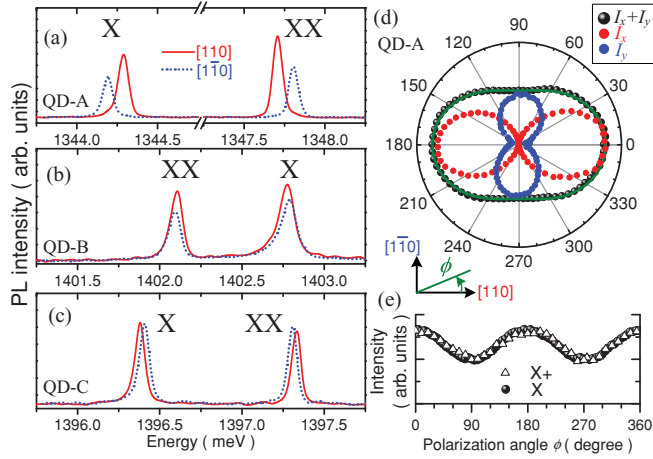


FIG. 1. (Color online) (a),(b),(c) Polarization resolved PL spectra along $[110]$ and $[1\bar{1}0]$ directions for three different QDs. (d) Polar plots of the intensities of the X doublet I_x , I_y and the total X -line intensity $I_x + I_y$ for QD-A as a function of the polarization angle ϕ . (e) A comparison between the polarization anisotropy of X and X^+ in QD-A.

high-energy component of X shows a stronger intensity. The total- X intensity exhibits a linear polarization degree $P_\ell \equiv (I_x - I_y)/(I_x + I_y)$ up to 26%, with a major polarization axis close to the x axis [Fig. 1(c)]. QD-B shows a smaller $P_\ell = 12\%$. The low-energy component of X now has a stronger intensity, while the major polarization axis remains close to the x axis. For QD-C, the PL intensity is nearly isotropic. The extracted P_ℓ is negative, but with a polarization degree below our detection accuracy ($\pm 2\%$). We consider $P_\ell \approx 0$ for this particular dot.

Figures 2(a) and (b) show the measured Δ_{FS} and P_ℓ as a function of the X -emission energy E_X for a series of QDs. A systematic decrease of Δ_{FS} with E_X and a reversal in sign when $E_X \gtrsim 1.4$ eV are observed. The sign of Δ_{FS} is closely related to the order of X and XX lines, as has been reported previously.^{30,31} In Fig. 2(b), a systematic decrease of P_ℓ with E_X is also observed, but only for $E_X < 1.4$ eV. For QDs with $E_X > 1.4$ eV, which are close to the wetting layer energy of 1.425 eV, P_ℓ are scattered. For all the investigated QDs (except QD-C), the major polarization axis aligns within $\pm 5^\circ$ along the x axis.

The physical origin of polarization anisotropy in QDs is a combined effect of the asymmetric confinement, strain anisotropy, piezoelectricity, as well as atomistic asymmetry.^{24–28} For a polarization degree up to 26%, the dominant source would be the dot-shape elongation, giving rise to an anisotropic envelop function elongated along the long axis. Theoretical calculations based on an empirical tight-binding approach^{27,28} predicted that a polarization degree up to 26% would correspond to a shape elongation ratio (L_x/L_y) at least up to ~ 1.7 . The decreasing P_ℓ in Fig. 2(b) thus indicates a reducing shape asymmetry with the reducing dot size. In Fig. 3(a), a plot of Δ_{FS} vs P_ℓ is displayed. We found that FSS is correlated with the polarization anisotropy for larger QDs emitting at $E_X < 1.4$ eV (solid symbols). However, no correlation was found for higher energy QDs (open symbols) near the wetting layer energy, indicating that

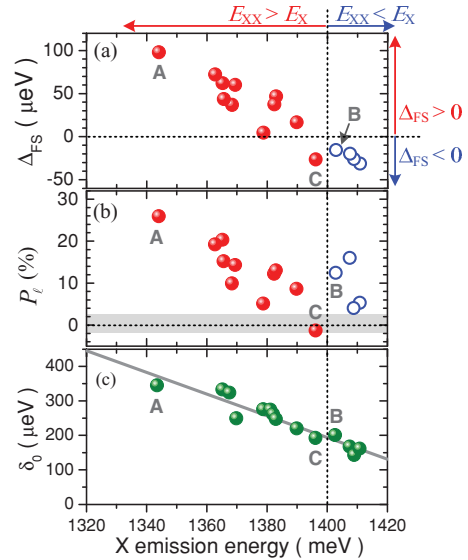


FIG. 2. (Color online) (a),(b) The measured Δ_{FS} and P_ℓ of X line as a function of E_X for a series of QDs. The data from QD-A, -B, and -C are also indicated. (c) The measured bright-to-dark X splitting δ_0 as a function of E_X .

the shape elongation for these weakly confined dots has no systematic size dependence.

If the dominant source of FSS is the long-range exchange interaction induced by an anisotropic envelop function, the low-energy component of X will be polarized along the dot elongation axis.^{32,33} Strikingly, our data suggest that, for those QDs with $\Delta_{FS} > 0$, the polarization direction of the low-energy X line is *perpendicular* to the major polarization axis defined by the elongation axis. Therefore, there must be a mechanism that tends to reverse the order of polarization eigenaxes, leading to the *anticorrelation* between FSS and polarization anisotropy.

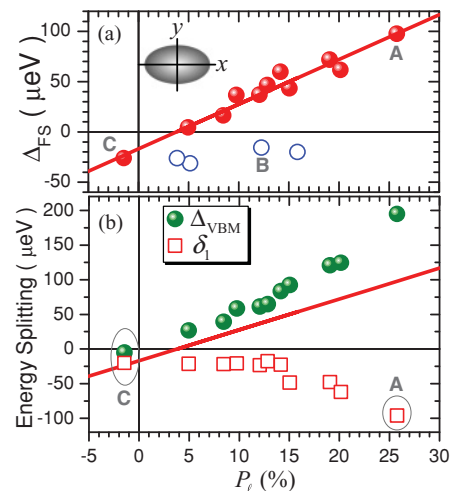


FIG. 3. (Color online) (a) The measured Δ_{FS} as a function of P_ℓ for the investigated QDs. The line is a linear fit to the data. (b) The estimated δ_1 and the VBM induced splitting $\Delta_{VBM} = 2P_\ell\delta_0$ as a function of P_ℓ . For clarity, data from weakly confined dots [open symbols in (a)] are excluded.

The polarization anisotropy can be described by the mixing between heavy-hole and light-hole states with projections of $J_z = \pm 3/2$ and $\pm 1/2$.^{24–26} Because the light-hole states are shifted in energy by the confinement and strain, the lowest hole state is still dominated by a heavy hole, with a light-hole component added as a perturbation, which reads as $|\psi_h^\pm\rangle \simeq |\pm 3/2\rangle - (\rho e^{\pm 2i\theta_p} / \Delta_{hl}) |\mp 1/2\rangle$, where Δ_{hl} is the heavy-light-hole energy splitting, ρ and θ_p are the strength and the phase of the mixing.³⁵ Because the light-hole component contributes a polarization opposite to that of the heavy hole, the resulting polarization will be elliptical with a linear polarization ratio $|P_\ell| = 2\gamma/(1 + \gamma^2)$ and a major polarization axis defined by θ_p , where $\gamma \equiv \frac{\rho}{\sqrt{3}\Delta_{hl}}$. From Fig. 2(b), we evaluate $\gamma \simeq 0-0.13$. The phase factor θ_p is associated with the off-diagonal elements in the Luttinger-Kohn and the Bir-Pikus Hamiltonians due to anisotropic confinement^{26,27} and strain,^{25,27} respectively. For strained InAs/GaAs QDs, since both the strain and confinement are associated with the shape asymmetry,²⁷ the resulting θ_p will thus align with the dot elongation axis.

Now we consider the influences of VBM on FSS. Restricting the consideration on the bright X subspace and considering the light-hole component as a perturbation, the effective spin Hamiltonian for the exchange interactions can be expressed as^{10,25,32,34}

$$\hat{H}_{\text{ex}}^X \simeq \frac{1}{2} \begin{pmatrix} \delta_0 & \delta_1 + 4\delta_0\tilde{\gamma} \\ \delta_1 + 4\delta_0\tilde{\gamma}^* & \delta_0 \end{pmatrix}, \quad (1)$$

in the basis of $|+1\rangle, |-1\rangle$, where δ_0 (δ_1) is the exchange splitting between the bright and dark states (the two bright states) of X with pure heavy-hole characters, and $4\delta_0\tilde{\gamma}$ with $\tilde{\gamma} = \gamma e^{-2i\theta_p}$ is induced by VBM due to the coupling of exchange splitting δ_0 via the light-hole admixture.^{25,34} Here, the effect of exchange interactions on VBM has been ignored. This can be verified from the polarization anisotropy of trion lines (X^+), which are identical to that of X lines in the same dot [Fig. 1(e)]. In the absence of light-hole mixing ($\gamma = 0$), the two bright X states coupled into $|x\rangle = \frac{|+1\rangle + |-1\rangle}{\sqrt{2}}$ and $|y\rangle = \frac{|+1\rangle - |-1\rangle}{\sqrt{2}}$ eigenstates, resulting in two equally intense emission lines separated by $\Delta_{\text{FS}} = E_x - E_y = \delta_1$. Since the dot shape and the envelop function are elongated along x , the long-range exchange interaction predicted that the low-energy eigenstate is $|x\rangle$,³² i.e., $\delta_1 < 0$. This is clearly contrary to our result of $\Delta_{\text{FS}} > 0$ shown in Fig. 2(a). In the presence of VBM ($\gamma \neq 0$), the intensities, FSS, and directions of polarization eigenaxes will be modified, as has been detailed in Ref. 25. For $\theta_p = 0^\circ$ according to the major polarization axis, FSS is given by

$$\Delta_{\text{FS}} \simeq \delta_1 + 4\delta_0\gamma. \quad (2)$$

Here, an additional splitting induced by VBM, $\Delta_{\text{VBM}} = 4\delta_0\gamma$, is added to (subtracted from) δ_1 when $P_\ell > 0$ ($P_\ell < 0$). Therefore, the lower-energy component of X is not necessary to be polarized along the QD long axis,^{25,34} contrary to the case where only pure heavy-hole states are considered.

To estimate Δ_{VBM} and δ_1 , we have measured the bright-to-dark splitting δ_0 by applying an in-plane magnetic field,^{10,11} which are shown in Fig. 2(c). Similar to Δ_{FS} , a systematic decrease of δ_0 with E_X is also observed. From the

deduced $\gamma \simeq P_\ell/2$, we estimate $\Delta_{\text{VBM}} \simeq 2P_\ell\delta_0$ and $\delta_1 \simeq \Delta_{\text{FS}} - \Delta_{\text{VBM}}$, which are shown in Fig. 3(b). Strikingly, we obtain a huge Δ_{VBM} , which appears to govern the overall size dependence of Δ_{FS} . All the estimated δ_1 are negative, consistent with the elongation direction predicted by the major polarization axis. This means that FSS in those QDs with significant shape elongation ($P_\ell > 5\%$) is dominated by the VBM induced splitting. It should be mentioned that both the measured P_ℓ and the coupling of δ_0 via VBM also depend on the overlap integrals of the electron, heavy-hole and light-hole envelop functions.³⁵ If the light hole is less confined, the actual VBM-induced splitting will be less than $2P_\ell\Delta_{\text{BD}}$. Nevertheless, even when the estimated Δ_{VBM} is reduced by a factor of two due to the less-confined light-hole envelops, the decreasing Δ_{FS} is still controlled by the decreasing Δ_{VBM} .

The VBM can be modified by an in-plane magnetic field \vec{B} through the Zeeman interactions on the electron and hole, which are given by^{10–12,24,25} $\hat{H}_B^X = \mu_B g_e \hat{S}_e \cdot \vec{B} - 2\mu_B (\kappa \hat{J}_h \cdot \vec{B} + q \hat{J}_h^3 \cdot \vec{B})$, where \hat{S}_e and \hat{J}_h are the electron and hole angular momentum operators, κ and q are Luttinger parameters. Since $\kappa \gg q$,^{10,24} the direct coupling between the heavy-hole states $|\pm 3/2\rangle$ via the \hat{J}_h^3 term is expected to be weak. However, if the linear term $\kappa \hat{J}_h \cdot \vec{B}$ dominates the Zeeman interaction, the magnetic coupling between the $|+1\rangle$ and $|-1\rangle$ bright X states can occur only through the light-hole admixture.^{12,24} In other words, the Zeeman interaction will affect FSS in a way similar to the coupling of exchange interactions through VBM. For simplicity, considering the light-hole component as a perturbation, the Zeeman interaction on the hole states ($|\psi_h^+\rangle, |\psi_h^-\rangle$) under a magnetic field $\vec{B} = B(\cos\varphi, \sin\varphi, 0)$ can be expressed as^{12,24} $\sum_{i,j} \tilde{\delta}_{h,i} \tilde{\delta}_{h,j} g_{ij}^h B_j$, where $\tilde{\delta}_{h,x} = -\hat{\sigma}_x/2$ and $\tilde{\delta}_{h,y} = \hat{\sigma}_y/2$ are the pseudospin operators ($\hat{\sigma}_i$: Pauli matrix); g_{ij}^h is the transverse hole g factor tensor, which is diagonal when the coordinate system is aligned with the major polarization axis, with $g_h = 12\kappa\gamma = -g_{xx}^h = g_{yy}^h$.

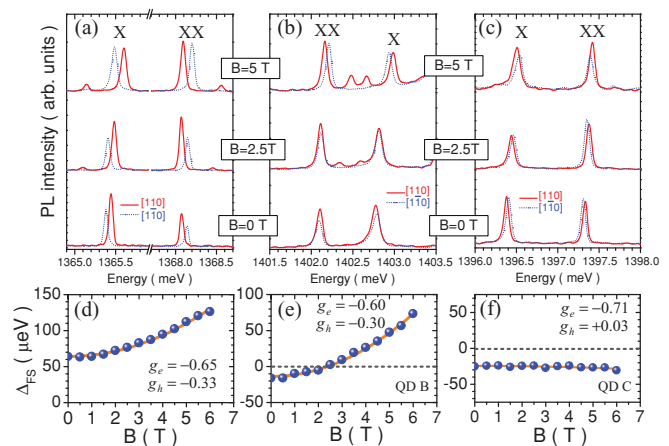


FIG. 4. (Color online) The measured magneto- μ PL spectra for three different QDs with (a) an initial $\Delta_{\text{FS}} > 0$, (b) an initial $\Delta_{\text{FS}} < 0$, and (c) an initial $\Delta_{\text{FS}} < 0$, but $P_\ell \approx 0$ (QD-C). (d),(e),(f) The corresponding Δ_{FS} as function of in-plane B shown in (a), (b), and (c), respectively. The in-plane g factors g_e and g_h deduced from $\mu_B(g_e \pm g_h)B$ are also indicated.

In the weak-field limit, the off-diagonal Zeeman terms can be further treated as perturbations to the bright states, which can be expressed as

$$\hat{H}_B^X \simeq \frac{\mu_B^2 B^2}{2\delta_0} \begin{pmatrix} \frac{1}{2}(g_e^2 + g_h^2) & g_e g_h \\ g_e g_h & \frac{1}{2}(g_e^2 + g_h^2) \end{pmatrix}. \quad (3)$$

Combining \hat{H}_{cx}^X and \hat{H}_B^X , we obtain

$$\Delta_{FS} \simeq \delta_1 + (4\delta_0 + \beta B^2)\gamma, \quad (4)$$

where $\beta = 12\kappa g_e \mu_B^2 / \delta_0$. It is thus clear that, depending on the sign of $g_e g_h$, a quadratic magnetic-field-induced splitting $\Delta_B(B) = \beta \gamma B^2$ will either add to ($g_e g_h > 0$) or subtract from ($g_e g_h < 0$) the initial FSS.

Figures 4(a) to 4(c) show the magneto- μ PL spectra for three QDs measured at different in-plane magnetic fields B . The corresponding FSS as a function of B are shown in Figs. 4(d) to (f). We found that the in-plane \vec{B} always increase the FSS for the investigated QDs with $P_\ell > 0$, as displayed in Fig. 4(a) and (b), indicating that g_e and g_h are of the same sign. This also explains why only those QDs with an initial negative FSS can be tuned to zero by an in-plane B , since the magnitude and sign of g_h are mainly determined by the strength and phase of VBM. As anticipated from Eq. (4), an in-plane B cannot affect the FSS without light-hole components ($\gamma = 0$) if the \hat{J}_h^3 term is negligible. This special case is shown in Fig. 4(c), where the measured Δ_{FS} for QD-C is almost unaffected by the applied B . The deduced g_h for QD-C is nearly zero because of $P_\ell \approx 0$ for this particular case. It is worth pointing out that this result is independent of the field direction φ , confirming the dominant contribution of the linear term $\kappa \hat{J}_h \cdot \vec{B}$ through VBM.

Due to the effect of VBM on FSS, the strategy for reducing FSS should further consider the way of reducing the heavy-light-hole mixing or eliminating the exchange coupling through VBM. Applying a uniaxial stress¹⁷⁻¹⁹ to modify both the strength and phase of VBM is very promising. However, the applied external perturbation must be aligned with the major axis defined by VBM. If a phase difference is present, the real and the imaginary parts of the off-diagonal elements in Eq. (1) cannot be eliminated simultaneously, leading to an anticrossing in the polarization eigenstates and a lower bound for FSS tuning.^{16,18,19} On the other hand, since the effect of an in-plane magnetic field on FSS has an identical phase with VBM [see Eq. (4)], a truly zero FSS can be achieved regardless the field direction.

IV. CONCLUSION

We observed a systematic correlation between the FSS and polarization anisotropy of an exciton in InAs/GaAs QDs, but with an unexpected reversal in order of the polarization eigenaxes. Such an anticorrelation indicates that the splitting induced by the exchange interactions coupled through VBM play an important role in the excitonic FSS in elongated QDs. This finding will impact the prospective strategy for FSS tuning by external perturbations.

ACKNOWLEDGMENTS

This work is supported in part by the program of MOE-ATU and the National Science Council of Taiwan under Grant No. NSC99-2112-M-009-008-MY2.

*whchang@mail.nctu.edu.tw

¹O. Benson, C. Santori, M. Pelton, and Y. Yamamoto, *Phys. Rev. Lett.* **84**, 2513 (2000).

²R. M. Stevenson, R. J. Young, P. Atkinson, K. Cooper, D. A. Ritchie, and A. J. Shields, *Nature (London)* **439**, 179 (2006).

³N. Akopian, N. H. Lindner, E. Poem, Y. Berlatzky, J. Avron, D. Gershoni, B. D. Gerardot, and P. M. Petroff, *Phys. Rev. Lett.* **96**, 130501 (2006).

⁴R. Hafenbrak, S. M. Ulrich, P. Michler, L. Wang, A. Rastelli, and O. G. Schmidt, *New J. Phys.* **9**, 315 (2007).

⁵R. J. Young, R. M. Stevenson, A. J. Hudson, C. A. Nicoll, D. A. Ritchie, and A. J. Shields, *Phys. Rev. Lett.* **102**, 030406 (2009).

⁶C. L. Salter, R. M. Stevenson, I. Farrer, C. A. Nicoll, D. A. Ritchie, and A. J. Shields, *Nature (London)* **465**, 594 (2010).

⁷A. Dousse, J. Suffczyński, A. Beveratos, O. Krebs, A. Lemaître, I. Sagnes, J. Bloch, P. Voisin, and P. Senellart, *Nature Phys.* **466**, 217 (2010).

⁸N. Gisin, G. Ribordy, W. Tittel, and H. Zbinden, *Rev. Mod. Phys.* **74**, 145 (2002).

⁹T. Jennewein, G. Weihs, J.-W. Pan, and A. Zeilinger, *Phys. Rev. Lett.* **88**, 017903 (2001).

¹⁰M. Bayer, G. Ortner, O. Stern, A. Kuther, A. A. Gorbunov, A. Forchel, P. Hawrylak, S. Fafard, K. Hinzer, T. L. Reinecke, S. N. Walck, J. P. Reithmaier, F. Klopff, and F. Schäfer, *Phys. Rev. B* **65**, 195315 (2002).

¹¹R. M. Stevenson, R. J. Young, P. See, D. G. Gevaux, K. Cooper, P. Atkinson, I. Farrer, D. A. Ritchie, and A. J. Shields, *Phys. Rev. B* **73**, 033306 (2006).

¹²K. Kowalik, O. Krebs, A. Golnik, J. Suffczyński, P. Wojnar, J. Kossut, J. A. Gaj, and P. Voisin, *Phys. Rev. B* **75**, 195340 (2007).

¹³K. Kowalik, O. Krebs, A. Lemaître, S. Laurent, P. Senellart, J. A. Gaj, and P. Voisin, *Appl. Phys. Lett.* **86**, 041907 (2005).

¹⁴B. D. Gerardot, D. Granados, S. Seidl, P. A. Dalgarno, R. J. Warburton, J. M. Garcia, K. Kowalik, O. Krebs, K. Karrai, A. Badolato, and P. M. Petroff, *Appl. Phys. Lett.* **90**, 041101 (2007).

¹⁵S. Marcet, K. Ohtani, and H. Ohno, *Appl. Phys. Lett.* **96**, 101117 (2010).

¹⁶A. J. Bennett, M. A. Pooley, R. M. Stevenson, M. B. Ward, R. B. Patel, A. Boyer de la Giroday, N. Skold, I. Farrer, C. A. Nicoll, D. A. Ritchie, and A. J. Shields, *Nature Phys.* **6**, 947 (2010).

¹⁷S. Seidl, M. Kroner, A. Högele, K. Karrai, R. J. Warburton, A. Badolato, and P. M. Petroff, *Appl. Phys. Lett.* **88**, 203113 (2006).

- ¹⁸J. D. Plumhof, V. Křápek, F. Ding, K. D. Jöns, R. Hafenbrak, P. Klenovský, A. Herklotz, K. Dörr, P. Michler, A. Rastelli, and O. G. Schmidt, e-print [arXiv:1011.3003](https://arxiv.org/abs/1011.3003) (2010).
- ¹⁹R. Singh and G. Bester, *Phys. Rev. Lett.* **104**, 196803 (2010).
- ²⁰T. Takagahara, *Phys. Rev. B* **62**, 16840 (2000).
- ²¹E. Kadantsev and P. Hawrylak, *Phys. Rev. B* **81**, 045311 (2010).
- ²²G. Bester, S. Nair, and A. Zunger, *Phys. Rev. B* **67**, 161306(R) (2003).
- ²³L. He, M. Gong, C.-F. Li, G.-C. Guo, and Alex Zunger, *Phys. Rev. Lett.* **101**, 157405 (2008).
- ²⁴A. V. Koudinov, I. A. Akimov, Yu. G. Kusrayev, and F. Henneberger, *Phys. Rev. B* **70**, 241305(R) (2004).
- ²⁵Y. Léger, L. Besombes, L. Maingault, and H. Mariette, *Phys. Rev. B* **76**, 045331 (2007).
- ²⁶T. Belhadj, T. Amand, A. Kunold, C.-M. Simon, T. Kuroda, M. Abbarchi, T. Mano, K. Sakoda, S. Kunz, and X. Marie, *Appl. Phys. Lett.* **97**, 051111 (2010).
- ²⁷W. Sheng, *Appl. Phys. Lett.* **89**, 173129 (2006).
- ²⁸W. Sheng and S. J. Xu, *Phys. Rev. B* **77**, 113305 (2008).
- ²⁹M.-F. Tsai, H. Lin, C.-H. Lin, S.-Di Lin, S.-Y. Wang, M.-C. Lo, S.-J. Cheng, M.-C. Lee, and W. -H. Chang, *Phys. Rev. Lett.* **101**, 267402 (2008).
- ³⁰R. Seguin, A. Schliwa, S. Rodt, K. Pötschke, U. W. Pohl, and D. Bimberg, *Phys. Rev. Lett.* **95**, 257402 (2005).
- ³¹R. J. Young, R. M. Stevenson, A. J. Shields, P. Atkinson, K. Cooper, D. A. Ritchie, K. M. Groom, A. I. Tartakovskii, and M. S. Skolnick, *Phys. Rev. B* **72**, 113305 (2005).
- ³²E. L. Ivchenko, *Phys. Status Solidi A* **164**, 487 (1997).
- ³³J. D. Plumhof, V. Křápek, L. Wang, A. Schliwa, D. Bimberg, A. Rastelli, and O. G. Schmidt, *Phys. Rev. B* **81**, 121309(R) (2010).
- ³⁴M. Z. Maialle, E. A. de Andrada e Silva, and L. J. Sham, *Phys. Rev. B* **47**, 15776 (1993).
- ³⁵For simplicity, we assume that the envelop functions for the heavy-hole (χ_{hh}) and light-hole (χ_{lh}) states are identical. If not, a factor of $\langle \chi_e \chi_{lh} \rangle / \langle \chi_e \chi_{hh} \rangle$ should be included in γ and a factor of $\langle \chi_e^2 \chi_{lh} \chi_{hh} \rangle / \langle \chi_e^2 \chi_{hh}^2 \rangle$ in $4\delta_0\gamma$, where χ_e is the electron envelop function. See Refs. 25 and 34.